Journal of
Ship&Ocean
Technology
©MARCH 2006

SOTECH Vol. 10, No. 1, pp. 10 ~ 26, 2006

A 3-Dimentional Radiation Diffraction Problem Analysis by B-Spline Higher-Order Panel Method

Gun-Do Kim [1] and Chang-Sup Lee [2]

[1] Maritime and Ocean Engineering Research Institute(MOERI), KORDI, Daejeon, Korea; E-mail: gdkim@moeri.re.kr
[2] Department of Naval Architecture and Ocean Engineering, Chungnam National University, Daejeon, Korea; E-mail: csleepro@cnu.ac.kr

Abstract

The radiation problem for oscillating bodies on the free surface has been formulated by the over-determined Green integral equation, where the boundary condition on the free surface is satisfied by adopting the Kelvin-type Green function and the irregular frequencies are removed by placing additional control points on the free surface surrounded by the body. The B-Spline based higher order panel method is then applied to solve the problem numerically. Because both the body geometry and the potential on the body surface are represented by the B-Splines, that is in polynomials of space parameters, the unknown potential can be determined accurately to the order desired above the constant value. In addition, the potential expressed in B-Spline can be differentiated analytically to get the velocity on the surface without introducing any numerical error. Sample computations are performed for a semispherical body and a rectangular box floating on the free surface for six-degrees of freedom motions. The added mass and damping coefficients are compared with those by the already-validated constant panel method of the same formulation showing strikingly good agreements.

Keywords: radiation problem, over-determined Green integral equation, B-spline, higher order panel method

1 Introduction

The three-dimensional radiation problem for oscillating bodies of arbitrary shape on the free surface has been studied by making use of a Green function satisfying the free surface condition known as the Kelvin-type Green function(John 1950). He has derived an integral equation, which is known as the Green integral equation where the potential on the body boundary surface is the unknown. He has also pointed out that the solution of the Green integral equation is not unique at certain frequencies known as the irregular frequencies. (Guevel et al 1978) have derived a Kelvin- type Green function and analyzed the same problem to solve the Green integral equation by making use of the constant panel method where the velocity potential is constant on a planar panel. The solution mentioned above has suffered difficulties in and around the irregular frequencies. (Kleinman 1982) has extended the region of integration for the Green integral equation to the waterplane, but could not prove the exactness of the solution. (Hong 1987) has derived an improved Green integral equation with symmetric kernel and proved the existence of the solution at the irregular frequencies. He has showed that accurate solution of the potential as well as its analytical derivative can be obtained at all frequencies including the irregular ones by making use of the constant panel method developed(Guevel et al 1978). (Hong 1987) also showed that the improved Green integral equation can be solved without the integral over the waterplane. It leads to an over-determined Green integral equation due to the non-symmetric kernel which can be solved in the least square sense(Hong and Lee 1999).

In this paper the higher order panel method(Lee and Kerwin 2003, Kim 2003) will be called HiPan to distinguish with the constant panel method(or the low order panel method, LoPan). It will be combined with the over-determined Green integral formulation(Hong 1987) to analyze the three-dimensional radiation problem. By adopting the HiPan, the geometry can be expressed more accurately and the number of panels required to discretize the surface will be smaller than the LoPan. To evaluate the new method, a hemispherical body and a rectangular box floating on the free surface are chosen. The computed results are then compared with those of the LoPan(Hong 1987). The comparison of velocity between the two methods is not presented in this paper. It will be presented in the calculation of drift force where the derivative of the potential plays an important role.

2 Intgral equation

We will choose a rectangular coordinate system as shown in Fig. 1 with the origin at the undisturbed free surface. The x- and y-axes are located on the free surface and the z-axis points vertically upward direction. The wetted surface is designated by S, the free surface by S_F and the waterline is designated by W. The body is in the 6-degrees of freedom motion with small amplitudes from the undisturbed mean position at the circular frequency of ω.

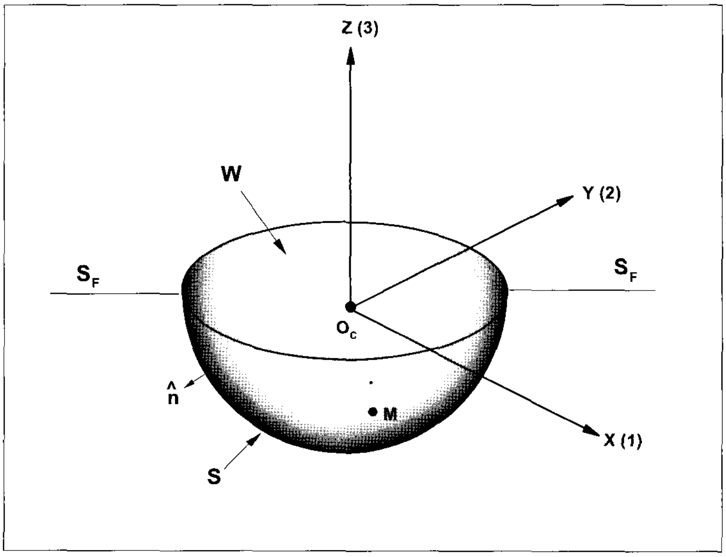

Fig. 1 Coordinate systems

The displacement of the point M on the body $\vec{A}_M$ from the mean position may be expressed as:

$$\vec{A}_M = \sum_{k=1}^{3} \mathrm{a}_k \vec{e}_k + \vec{\theta} \times \overrightarrow{O_c M}$$
$$\vec{\theta} = \sum_{k=1}^{3} \theta_k \vec{e}_k = \sum_{k=4}^{6} \mathrm{a}_k \vec{e}_{k-3} \tag{1}$$

where O_c is the center of rotation of the body and a_k the amplitudes of the 6-degrees of freedom motions and are expressed as:

$$\begin{aligned} \mathrm{a}_k &= \mathrm{a}_k^* \cos \omega t + \mathrm{a}_k^{**} \sin \omega t \\ &= \mathrm{Re}\{a_k e^{-i\omega t}\}, \quad k = 1,2,...,6 \end{aligned} \tag{2}$$

where $a_k = \mathrm{a}_k^* + i\mathrm{a}_k^{**}$ is the complex motion amplitude. The velocity of the fluid around the body can be obtained by taking the derivative of the velocity potentials as follows:

$$\Phi_R = \mathrm{Re}\{\phi_R e^{-i\omega t}\}$$
$$\phi_R = -i\omega \sum_{k=1}^{6} a_k \phi_k \tag{3}$$

where ϕ_R is the complex radiation potential. The complex valued potential will be computed for the body in motion with the unit amplitude; that is, the body velocity is assumed to be $1 \cdot \cos \omega t$ without losing generality. The complex motion amplitude a_k is determined by solving the equation of the motion in the frequency domain, which is beyond the scope of the present paper.

2.1 Boundary conditions for the velocity potential ϕ_k

For motion of small amplitudes, the boundary condition on the body surface may be applied on the mean position of the body as:

$$-k_0 \phi_k + \frac{\partial \phi_k}{\partial z} = 0 \tag{4}$$

$$\frac{\partial \phi_k}{\partial n} = \vec{e}_k \cdot \vec{n}_M \quad on \ \ S, \ \ k = 1,2,3 \tag{5}$$

$$\frac{\partial \phi_k}{\partial n} = (\vec{e}_{k-3} \times \overrightarrow{O_c M}) \cdot \vec{n}_M \quad on \ \ S, \ \ k = 4,5,6 \tag{6}$$

where S denotes the wetted surface and $k_0 = \omega^2 / g$ the wave number, g the gravitational acceleration. The potential should satisfy the radiation condition at infinity.

We will use the Kelvin-type Green function $G(P, M;\ k_0)$ of (Guevel et al 1978) which satisfies the free surface boundary condition (4) and the radiation condition, and then can express the velocity potential ϕ_k in the form of the Green integral equation as:

$$\frac{\phi_k}{2}+\int_S \phi_k(M)\frac{\partial G(P,M;k_0)}{\partial n_M}dS_M \\ =\int_S \frac{\partial \phi_k(M)}{\partial n_M}G(P,M;k_0)dS_M,\ P\ \ on\ \ S\cup W \tag{7}$$

where P and M designate the field point and the source point, respectively.

3 Discretization of integral equation using B-splines

The geometry of the body may be expressed using B-Splines (Piegl and Tiller 1996) as:

$$\vec{x}(u,v)=\sum_{i,j}\overrightarrow{x^v}_{i,j}\cdot\tilde{N}_i(u)\cdot\tilde{M}_j(v) \tag{8}$$

where $\vec{x}(u,v)$ denotes the B-Spline-represented surface, $\tilde{N}_i(u)$ *and* $\tilde{M}_j(v)$ are the B-Spline basis functions in the parametric spaces u and v, respectively, and $x^v{}_{i,j}$ is the coordinates of the control vertices.

The velocity potential ϕ may also be expressed in the same manner as:

$$\phi=\sum_{i,j}\phi^v{}_{i,j}N_i(u)M_j(v) \tag{9}$$

where $\phi^v{}_{i,j}$ is the control vertices to represent the potential in B-Splines. $N_i(u)$ *and* $M_j(v)$ are the B-Spline basis functions. It should be noted that the extent of the parametric spaces u and v in (8) and (9) should coincide each other. We drop the subscript k from the velocity potential ϕ_k used to distinguish the mode of motions without losing the clarity. Because the problem is linear, the general solution will be the linear combination of solutions to each mode.

We first discretize (7) in parametric spaces of u and v, and substitute (9) into (7) to obtain the following:

$$\frac{1}{2}\left\{\sum_{i,j}\phi^v{}_{i,j}N_i(u)M_j(v)\right\}+\sum_{v,\mu}\int_{S_{v,\mu}}\left\{\sum_{i,j}\phi^v{}_{i,j}N_i(u)M_j(v)\right\}\frac{\partial G}{\partial n}dS=\sum_{v,\mu}\int_{S_{v,\mu}}\frac{\partial \phi}{\partial n}GdS \tag{10}$$

Rearranging the order of integration and the summation over the potential vertices in the second term of (10), we will obtain the following:

$$\frac{1}{2}\left\{\sum_{i,j}\phi^v{}_{i,j}N_i(u)M_j(v)\right\}+\sum_{v,\mu}\sum_{i,j}\phi^v{}_{i,j}\int_{S_{v,\mu}}N_i(u)M_j(v)\frac{\partial G}{\partial n}dS=\sum_{v,\mu}\int_{S_{v,\mu}}\frac{\partial \phi}{\partial n}GdS \tag{11}$$

The above equation is similar to the Green integral equation in LoPan, but differs in the form of the integrand; especially the dipole induction integral has weight function formed by the product of two B-Spline basis functions $N_i(u)$ *and* $M_j(v)$ and the integration is performed in the parametric spaces. Details to compute the induction integrals may be found in (Kim 2003), and will not be repeated here.

4 Computation of hydrodynamic forces

Once the potential is known, the radiation force and moment acting on the wetted surface of the floating body can be computed as:

$$\vec{F} = -i\rho\omega \int_S \phi_R \vec{n} dS \tag{12}$$

$$\vec{M} = -i\rho\omega \int_S \overrightarrow{O_c M} \times \phi_R \vec{n} dS \tag{13}$$

The dimension of ϕ_1, ϕ_2 and ϕ_3 is L, where L is the characteristics length, and the dimension of ϕ_4, ϕ_5 and ϕ_6 is L^2. All the physical quantities are nondimensionalized as:

$$\begin{aligned} &X = \frac{x}{L},\ Y = \frac{y}{L},\ Z = \frac{z}{L} \\ &\tilde{\phi}_k = \frac{\phi_k}{L},\ k = 1,\ 2,\ 3 \\ &\tilde{\phi}_k = \frac{\phi_k}{L^2},\ k = 4,\ 5,\ 6 \end{aligned} \tag{14}$$

Substituting (3) into (12) and (13) will lead to the following:

$$\vec{F} = -\rho\omega^2 \sum_{k=1}^{6} a_k \int_S \phi_k \vec{n} dS \tag{15}$$

$$\vec{M} = -\rho\omega^2 \sum_{k=1}^{6} a_k \int_S \overrightarrow{O_c M} \times \phi_k \vec{n} dS \tag{16}$$

The forces may now be expressed in terms of the added mass coefficient m_{jk}, the $j-$directional force due to the $k-$directional motion, and similarly-defined wave damping coefficient D_{jk} as:

$$\vec{F} = \sum_{j=1}^{3} F_j \vec{e}_j \tag{17}$$

$$F_j = -\rho\omega^2 L^q \sum_{k=1}^{6} (m_{jk} + iD_{jk}) a_k,\ \begin{cases} q = 3,\ k = 1,\ 2,\ 3 \\ q = 4,\ k = 4,\ 5,\ 6 \end{cases} \tag{18}$$

Similarly the moments are now expressed by

$$\vec{M} = \sum_{j=1}^{3} M_j \vec{e}_j \tag{19}$$

$$M_j = -\rho\omega^2 L^q \sum_{k=1}^{6} (m_{jk} + iD_{jk}) a_k,\ \begin{cases} q = 4,\ k = 1,\ 2,\ 3 \\ q = 5,\ k = 4,\ 5,\ 6 \end{cases} \tag{20}$$

The added mass coefficients may now be expressed as:

$$m_{jk} = -\text{Re}\{\int \tilde{\phi}_k n_j d\tilde{S}\}, \ \ j = 1,\ 2,\ 3 \tag{21}$$

$$m_{jk} = -\text{Re} \int \left(\frac{\overrightarrow{O_c M}}{L} \times \vec{n} \right) \cdot \vec{e}_{j-3} \tilde{\phi}_k d\tilde{S}, \ \ j = 4,\ 5,\ 6 \tag{22}$$

The wave damping coefficients may now be expressed as:

$$D_{jk} = -\text{Im}\{\int \tilde{\phi}_k n_j d\tilde{S}\}, \ \ j = 1,\ 2,\ 3 \tag{23}$$

$$D_{jk} = -\text{Im} \int \left(\frac{\overrightarrow{O_c M}}{L} \times \vec{n} \right) \cdot \vec{e}_{j-3} \tilde{\phi}_k d\tilde{S}, \ \ j = 4,5,6 \tag{24}$$

5 Results and discussions

To evaluate the new formulation, a hemisphere with the diameter $D = 1$ is chosen for numerical computation. This body is simple enough in shape and has been tested by previous works, and hence is proper as the first example to check the numerical algorithm. Convergence on the discretization is first demonstrated in Figures 2 and 3, where the number of panels in the parametric u and v directions is doubled showing the graphically indistinguishable differences in the added mass and damping coefficients for the sphere in sway motion at two selected wave numbers $K = k_0 D$. Assuming the convergence is achieved, the number of panels combination in both parametric directions is chosen to be 12×6 in all the subsequence computations.

Figures 4 and 5 show the added mass and damping coefficients for the hemisphere in heave as a function of wave number. Computations are first made in accordance with the most-commonly known Green integral formulation without any control points on the free surface. It may be observed that at a wave number (in this case at $K = 5.13$) the computed force coefficients show spikes in the present HiPan formulation. This is the well-known irregular frequency phenomenon. It is clearly seen that the present formulation, which locates the control points on the free surface inside the body following (Hong 1987) in addition to the traditional control points on the wetted body surface, eliminates the irregular frequency completely. The similar computations are made for the hemisphere in the sway motion and the results are shown in Figures 6 and 7. The same observation can be made for this sway motion as in the heave motion. We see that the irregular frequencies are present in the higher order panel methods, too, but can be removed completely by the over-determined Green integral equation formulation.

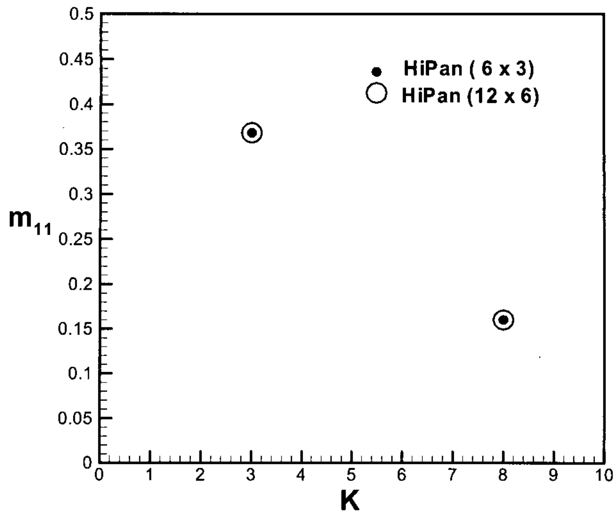

Fig. 2 Comparison of sway added mass coefficients computed by present method for two different sets of panel numbers at selected wave numbers

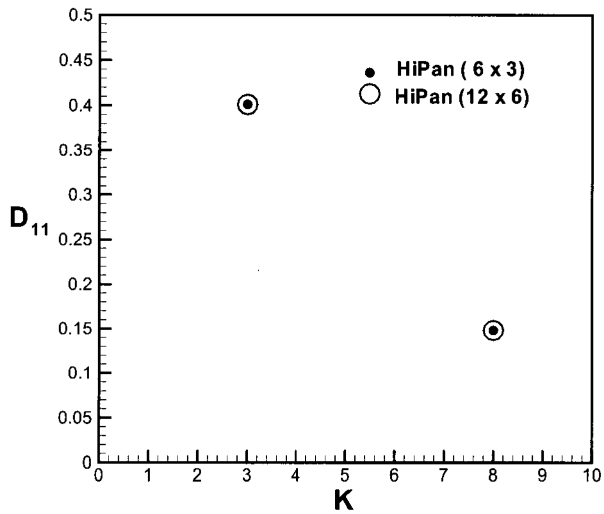

Fig. 3 Comparison of sway damping coefficients computed by present method for two different sets of panel numbers at selected wave numbers

To validate the present higher order panel method, the computational results made for the heave and sway motions are compared with those already-proved low order panel method as shown in Figures 8 through 11. In both formulations the over-determined Green integral equation is adopted.

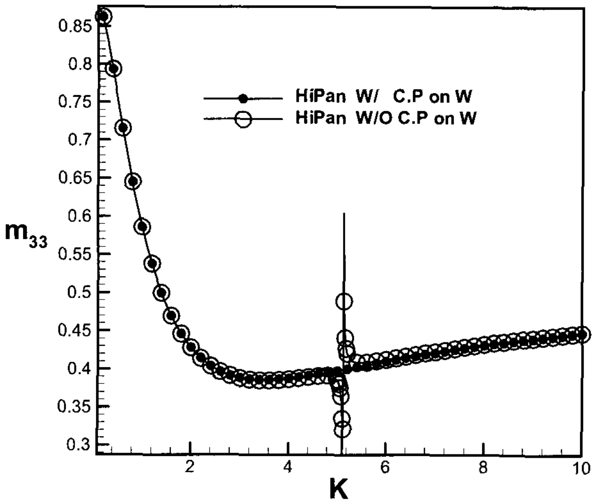

Fig. 4 Heave added mass coefficients versus wave numbers computed by present method. Note the irregular frequency present at K=5.13 in traditional Green integral formulation

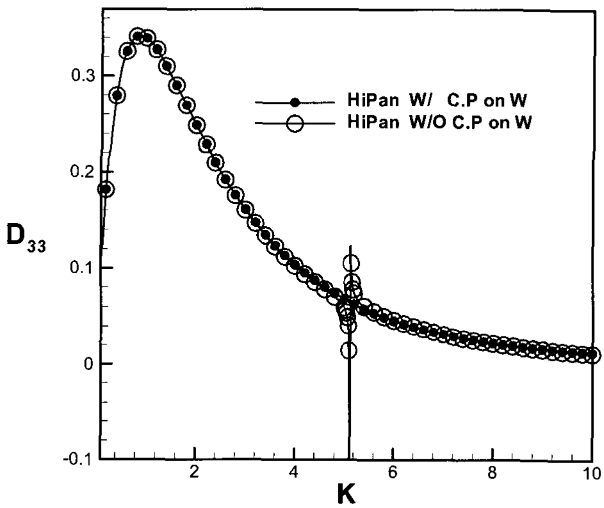

Fig. 5 Heave wave damping coefficients versus wave numbers computed by present method. Note the same irregular frequency present as in Fig. 4

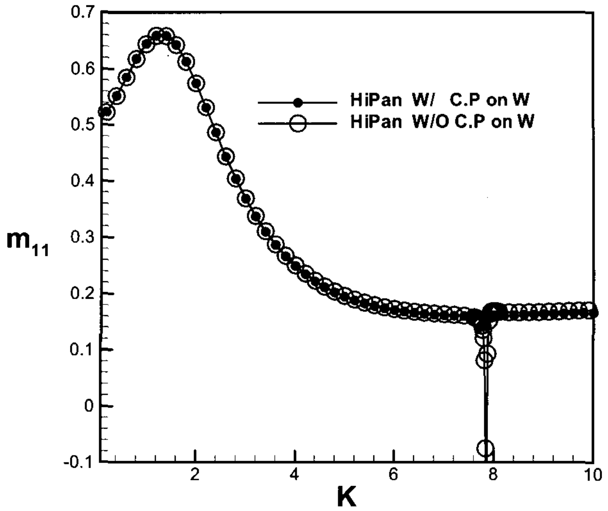

Fig. 6 Sway added mass coefficients versus wave numbers computed by present method. Note the irregular frequency present at K=7.86 in traditional Green integral formulation

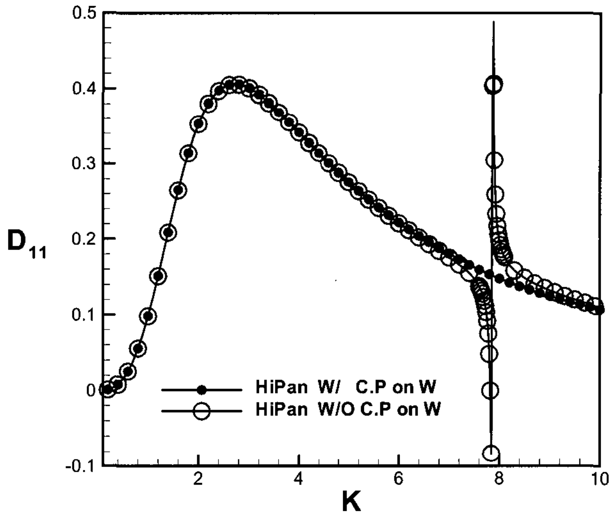

Fig. 7 Sway wave damping coefficients versus wave numbers computed by present method. Note the same irregular frequency present as in Fig. 6

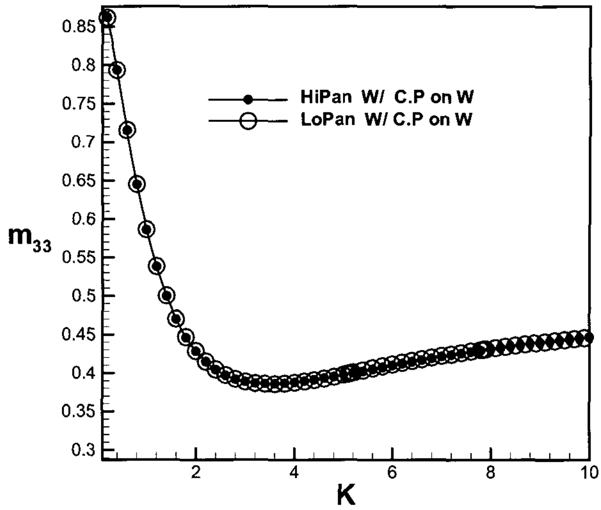

Fig. 8 Comparison of heave added mass coefficients versus wave numbers computed by HiPan and LoPan. In both methods the over-determined Green integral formulation is adopted

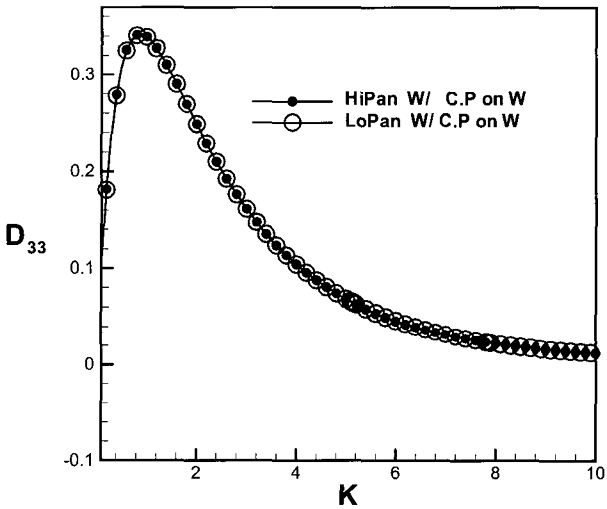

Fig. 9 Comparison of heave wave damping coefficients versus wave numbers computed by HiPan and LoPan. In both methods the over-determined Green integral formulation is adopted

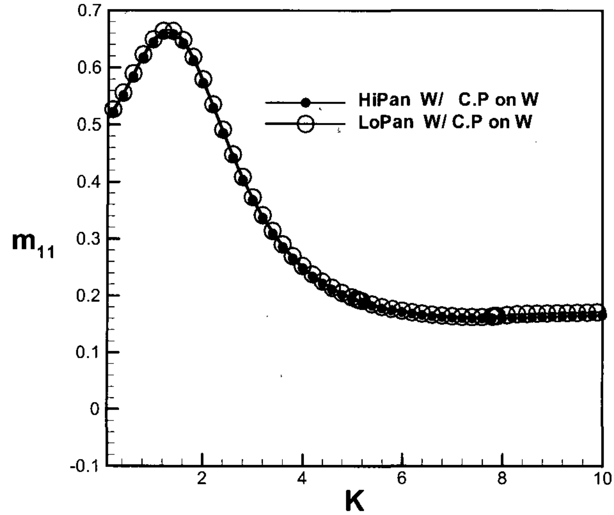

Fig. 10 Comparison of sway added mass coefficients versus wave numbers computed by HiPan and LoPan. In both methods the over-determined Green integral formulation is adopted

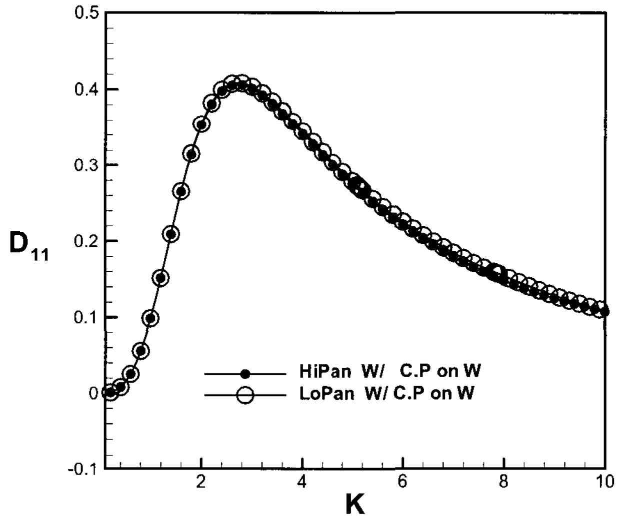

Fig. 11 Comparison of sway wave damping coefficients versus wave numbers computed by HiPan and LoPan. In both methods the over-determined Green integral formulation is adopted

And also numerical computation is performed for rectangular box with the dimensions($L \times B \times T = 10 \times 10 \times 2$). Figure 12 shows facet representation of the rectangular box.

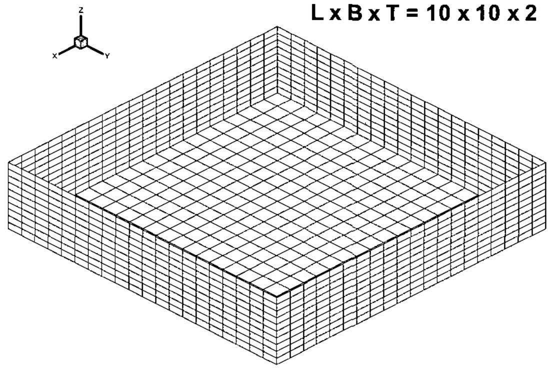

Fig. 12 Facet representation of rectangular box

Figures 13 and 14 show the added mass and damping coefficients for the box in heave as a function of wave number. Here the non-dimensional wave number is defined as $K = k_0 L$ for the rectangular box. Computations are first made in accordance with the most-commonly known Green integral formulation without any control points on the free surface. It may be observed that at a wave number (in this case at K =6.25) the computed force coefficients show spikes in the present HiPan formulation. The similar computations are made for the box in the sway motion and the results are shown in Figs. 15 and 16. The same observation can be made for this sway motion as in the heave motion. We see that the irregular frequencies are present in the higher order panel methods, too, but can be removed completely by the over-determined Green integral equation formulation.

To validate the present higher order panel method, the computational results made for the heave and sway motions are compared with those already-proved low order panel method as shown in Figs. 17 through 20. In both formulations the over-determined Green integral equation is adopted.

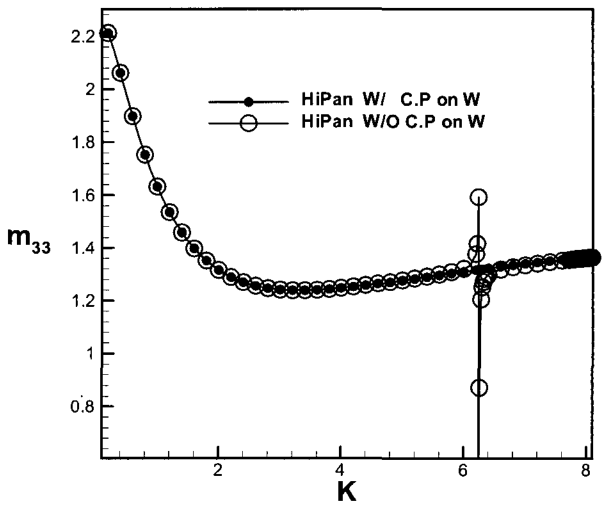

Fig. 13 Heave added mass coefficients versus wave numbers for a floating box computed by present method

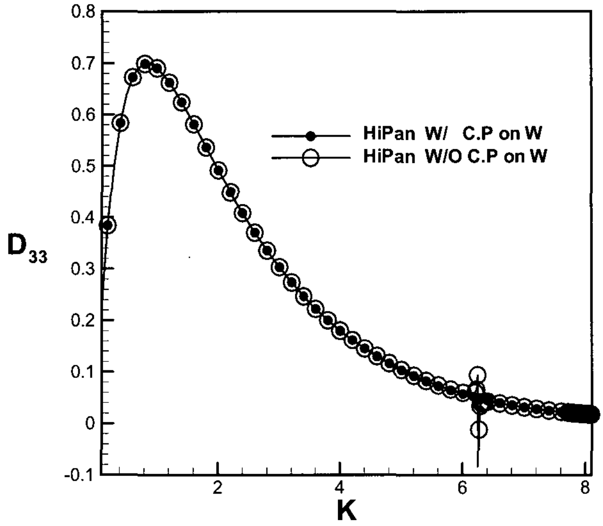

Fig. 14 Heave wave damping coefficients versus wave numbers for a floating box computed by present method

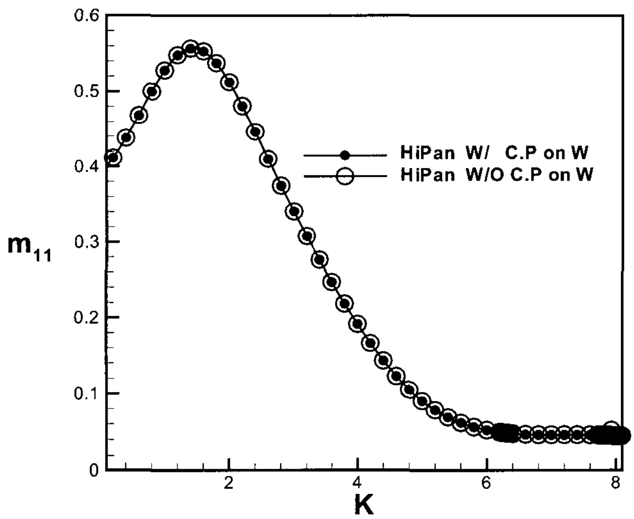

Fig. 15 Sway added mass coefficients versus wave numbers for a floating box computed by present method

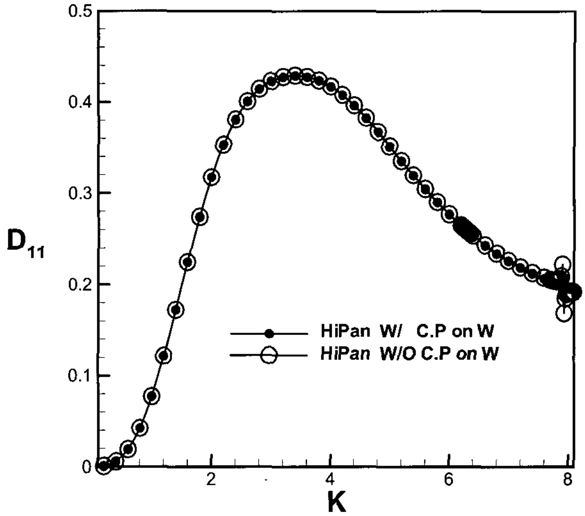

Fig. 16 Sway wave damping coefficients versus wave numbers for a floating box computed by present method

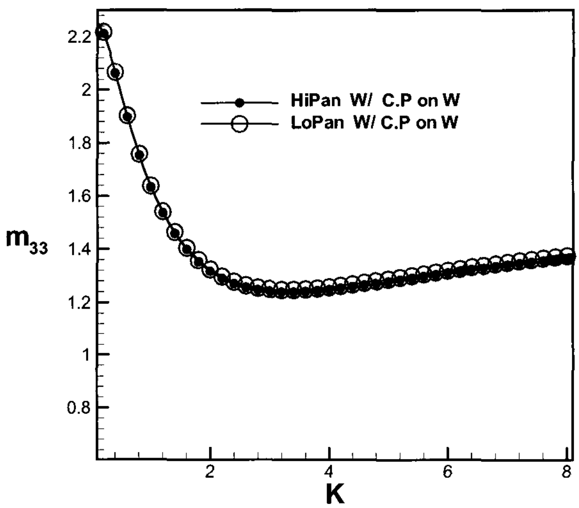

Fig. 17 Comparison of heave added mass coefficients versus wave numbers for a floating box computed by HiPan and LoPan. In both methods the over-determined Green integral formulation is adopted

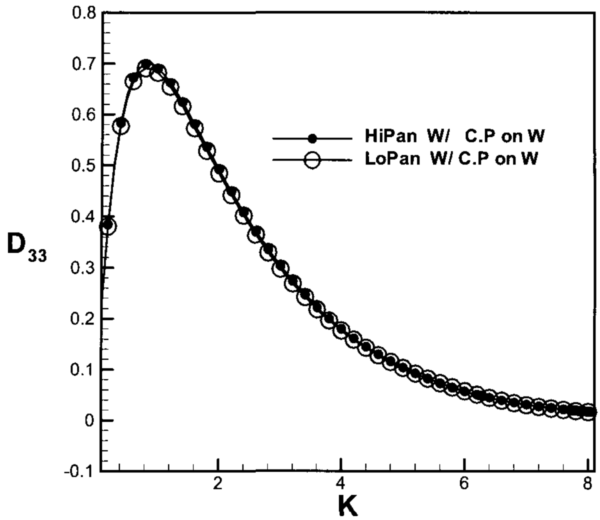

Fig. 18 Comparison of heave wave damping coefficients versus wave numbers for a floating box computed by HiPan and LoPan. In both methods the over-determined Green integral formulation is adopted

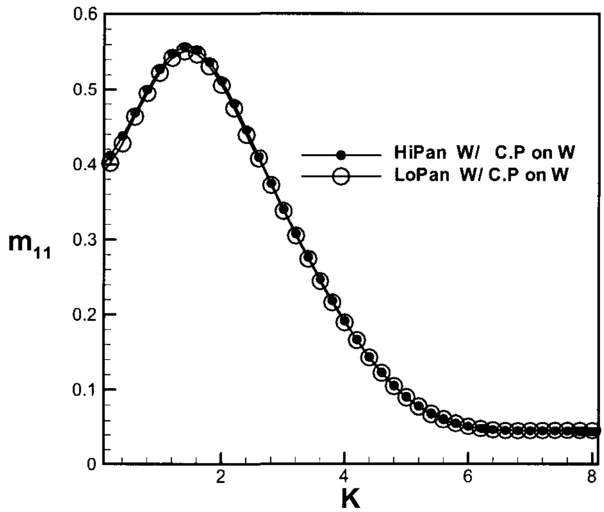

Fig. 19 Comparison of sway added mass coefficients versus wave numbers for a floating box computed by HiPan and LoPan. In both methods the over-determined Green integral formulation is adopted

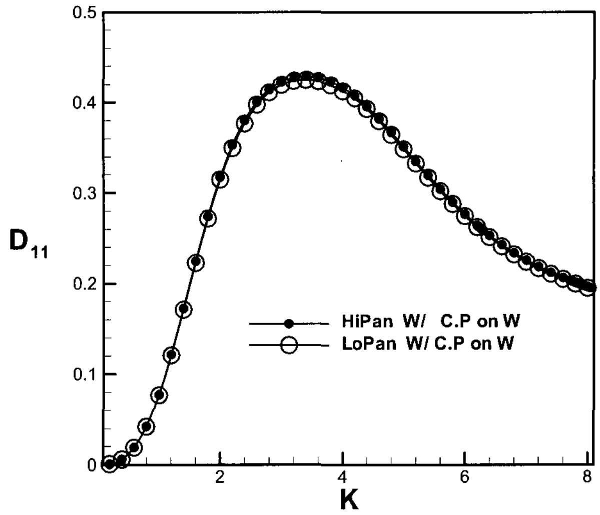

Fig. 20 Comparison of sway wave damping coefficients versus wave numbers for a floating box computed by HiPan and LoPan. In both methods the over-determined Green integral formulation is adopted

6 Conclusions

A B-Spline higher order panel method based on the over-determined Green integral equation is formulated and is proved to produce accurate added mass and damping coefficients in the radiation problem with the irregular frequencies removed completely.

The B-Spline based higher order panel method is validated to give the same results as the low order panel method, when both methods are formulated based on the same over-determined Green integral formulation.

It is shown that smaller number of panels could provide the same accuracy as the low order panel method.

Because the derivative to any order can be taken analytically in the higher order panel method, the new method can be used for prediction of the drift forces requiring more accurate second order computation.

References

John, F. 1950. On the motion of floating bodies II. Communications on Pure and Applied Mathematics, No.3, pp.45-101.

Guevel, P., J.C. Daubisse and G. Delhommeau. 1978. Oscillations des corps flottants soumis aux action de la houle. Bulletin de l'ATMA, Paris, Paper No. 1808.

Kleinman, R.E. 1982. On the mathematical theory of motion of floating bodies-An update. Report DTNSRDC-82/074.

Hong, D.C. 1987. On the improved Green integral equation applied to the water-wave radiation-diffraction problem. J. Society of Naval Architect of Korea Vo.24, No.1, pp.1-8.

Hong, D.C. and C.S. Lee. 1999. A B-Spline Higher Order Panel Method Applied to the

Radiation Wave Problem for a 2-D Body Oscillating on the Free Surface. Journal of Ship and Ocean Technology, Vol.3, No.4, pp.1-14.

Lee, C.S. and J.E. Kerwin. 2003. A B-Spline Higher Order Panel Method Applied to Two-Dimensional Lifting Problem. Journal of Ship Research, Vol.47, No.4, pp.290-298.

Kim, G.D. 2003. Application of High Order Panel Method for Improvement of Prediction of Marine Propeller Performance. PhD Thesis, Department of Naval Architecture and Ocean Engineering, Chungnam National University.

Piegl, L. and W. Tiller. 1996. The NURBS Book, 2nd Ed. Springer-Verlag. Berlin, Heidelberg.